Title

A Mutated Anti-CA19-9 scFv-Fc for Positron Emission Tomography of Human Pancreatic Cancer Xenografts

Journal

Molecular Imaging and Biology, 16(5)

ISSN

1536-1632

Authors

Rochefort, Matthew M
Girgis, Mark D
Knowles, Scott M
et al.

Publication Date

2014-10-01

DOI

10.1007/s11307-014-0733-4

Peer reviewed

MOLECULAR IMAGING AND BIOLOGY

Mol Imaging Biol (2014) 16:721–729
DOI: 10.1007/s11307-014-0733-4

Published Online: 2 April 2014

World Molecular Imaging Society

RESEARCH ARTICLE

A Mutated Anti-CA19-9 scFv-Fc for Positron Emission Tomography of Human Pancreatic Cancer Xenografts

Matthew M. Rochefort,[1,2] Mark D. Girgis,[1,2] Scott M. Knowles,[3] Jacob S. Ankeny,[1,2] Felix Salazar,[3] Anna M. Wu,[3] James S. Tomlinson[1,2]

[1]*Department of Surgery, UCLA, 570 Westwood Plaza, Bldg 114, CNSI, Rm4324E, Los Angeles, CA, 90095, USA*
[2]*Department of Surgery, Veterans Healthcare Affairs, Greater Los Angeles, Los Angeles, CA, USA*
[3]*Crump Institute for Molecular Imaging, Department of Molecular and Medical Pharmacology, UCLA, 570 Westwood Plaza, Bldg 114, CNSI, Rm4324E, Los Angeles, CA, 90095, USA*

Abstract

Purpose: Intact antibodies have a long serum persistence resulting in high background signal that inhibits their direct translation as imaging agents. Engineering of antibody fragments through the introduction of mutations in the fragment crystallizable (Fc) region can dramatically reduce serum persistence. We sought to develop a Fc-mutated, anti-CA19-9 antibody fragment (anti-CA 19-9 scFv-Fc H310A) to provide micro-positron emission tomography (microPET) imaging of pancreatic cancer xenografts.

Procedures: The anti-CA19-9 scFv-Fc H310A was successfully expressed and purified. Biochemical characterization included size exclusion chromatography, sodium dodecyl sulfate polyacrylamide gel electrophoresis (SDS-PAGE), Western blot, and flow cytometry. The antibody fragment was labeled with iodine-124 (^{124}I) and injected into mice containing human pancreatic cancer xenografts. MicroPET/CT images were then obtained. Blood, organ, and tumor radioactivity was measured and expressed as the percent of injected dose per gram of tissue (%ID/g).

Results: Biochemical characterization was consistent with the creation of a 105 kD dimer containing a human Fc region. Flow cytometry demonstrated antigen-specific binding, and cell-based ELISA further established a dissociation constant (K_D) of 10.7 nM. ^{124}I-labeled scFv-Fc H310A localized to the antigen-positive tumor xenografts as detected by microPET. Objective confirmation of targeting was demonstrated by higher %ID/g in the antigen-positive tumor compared to the blood, antigen-negative tumor, and liver.

Conclusions: We successfully engineered and produced an anti-CA19-9 scFv-Fc H310A antibody fragment that retains similar affinity when compared to the parental intact murine antibody. Additionally, our engineered and mutated fragment exhibited antigen-specific microPET imaging of both subcutaneous and orthotopic pancreatic cancer xenografts at early time points secondary to decreased serum half-life.

Key Words: Pancreas, Cancer, CA 19-9, Imaging, Antibody, scFv-Fc

Correspondence to: James Tomlinson; *e-mail:* jtomlinson@mednet.ucla.edu

Introduction

Pancreatic cancer is the fourth leading cause of cancer-related mortality in the US. With almost 44,000 new diagnoses and 37,000 deaths attributed to pancreatic cancer in 2012, it has a mortality that approximates its incidence [1]. The very high mortality rate for pancreatic cancer is due, in part, to the nonspecific nature of the early symptoms [2] leading to delay in diagnosis and the resulting poor patient outcomes with an overall 5-year survival of only 6 % [3]. The only hope for cure in pancreatic cancer is surgical resection; however, only 20 % of patients are eligible for resection at the time of diagnosis [4], and those patients still have a 5-year survival of only 18–25 %, due to occult micrometastatic disease [2, 5, 6]. Given our current inability to detect the extent of disease in pancreatic cancer, the majority of patients are routinely understaged and may undergo operations with significant morbidity and mortality without any survival benefit. These data indicate the need for the development of novel strategies for tumor-specific imaging and targeted therapeutics of micrometastatic and disseminated disease.

Monoclonal antibodies posses exquisite antigen specificity and therefore have the potential to be utilized both as tumor-specific imaging agents as well as targeted therapeutics [7]. In this sense, the ability of the antibody to function as an imaging agent is a surrogate for its ability to localize to the tumor and function as a therapeutic agent. When labeled with a radionuclide and utilized as a positron emission tomography (PET) imaging agent (immunoPET), antibodies directed against cell surface tumor antigens have the ability to provide sensitive and specific imaging of a cancer. The efficacy of monoclonal antibodies as PET imaging agents depends in part on the nature of the targeted antigen. The ideal antigen should be absent on normal tissue, abundant on cancerous tissue, and expressed on the cell surface so that it is accessible [8].

For pancreatic cancer, one such antigen is the cell surface carbohydrate antigen known as CA 19-9. It is among the most highly expressed tumor-associated antigens, present on over 90 % of all resected pancreatic tumors [9–11] and has very low levels of expression on normal pancreatic ductal cells, where it is spatially limited to the apical membrane [12]. These characteristics make CA 19-9 a favorable candidate for targeted molecular imaging of pancreatic cancer [13]. Our lab previously investigated the utility of an anti-CA19-9 intact murine antibody as an imaging agent for pancreatic cancer in a subcutaneous mouse xenograft model and demonstrated robust target specificity [14]. However, the prolonged serum half-life of the intact antibody necessitated delayed image acquisition to provide for adequate tumor to background contrast for effective tumor visualization. We determined that the prolonged half-life was an area of potential improvement for clinical translation. A reduction in serum half-life should allow for earlier image acquisition due to the reduced background signal.

One of the most common methodologies for overcoming the lengthy serum persistence of an intact antibody is to reduce its size. Our lab and others have produced antibodies with one or more domains deleted from the final product. These include the diabody (dimer of the VH and VL domains), minibody (dimer of the VH, VL, and CH3 domains), and single-chain Fv-Fc (dimer of the VH, VL, CH2, and CH3 domains). Our lab has previously investigated the utility of the scFv-Fc fragment due to its ease of production and stability [15]. Moreover, it possess an intact fragment crystallizable (Fc) region into which mutations can be introduced to modulate the half-life of the fragment through alteration of amino acids in the C_H2-C_H3 region found to be paramount to the Fc-FcRn binding which prevents lysosomal degradation [16, 17]. This allows the scFv-Fc antibody fragment to be modified by a point mutation, resulting in a pharmacokinetic profile more suited for imaging. This paper represents our initial efforts of creating and characterizing a mutated (histidine at position 310 to alanine) scFv-Fc antibody fragment against the cell surface pancreatic cancer epitope CA 19-9. *In vitro* characterization of our antibody fragment included antigen-specific cell targeting via flow cytometry and antibody-antigen affinity assessment through cell-based ELISA. Additionally, we assessed the *in vivo* characteristics of our mutated antibody fragment including serum half-life, subcutaneous and orthotopic murine pancreatic cancer xenograft imaging via immunoPET, and quantitative biodistribution of tumor and organ uptake.

Materials and Methods

Design and Gene Assembly

The anti-CA 19-9 single-chain variable region (scFv) is composed of the murine V_L gene and murine V_H gene previously constructed for the creation of a diabody [18] connected by an 18-amino-acid peptide linker [19]. This scFv was then fused to the C_H2 and C_H3 domains of the human IgG1. The final product consists of a single chain containing the murine V_H and V_L and the human C_H2 and C_H3 domains, a chimeric scFv-Fc monomer, which when produced, dimerizes to produce the final scFv-Fc antibody fragment (Fig. 1a).

A single mutation was introduced to the DNA sequence of the human C_H2 domain converting $histidine_{310}$ to an alanine as described previously [20] to create the final scFv-Fc H310A antibody fragment (scFv-Fc H310A). The scFv-Fc H310A sequence was assembled in a p-MA plasmid containing the native mammalian expression leader sequence by GeneArt (Life Technologies, Grand Island, NY). The sequence was excised from the p-MA vector and ligated into the pEE12 mammalian expression vector (Lonza Biologics, Slough, UK) containing the glutamine synthetase gene. The primary amino acid sequences obtained from DNA sequence analyses of cloned isolates were compared with the parental murine 1116-NS-19-9 DNA sequence prior to expression.

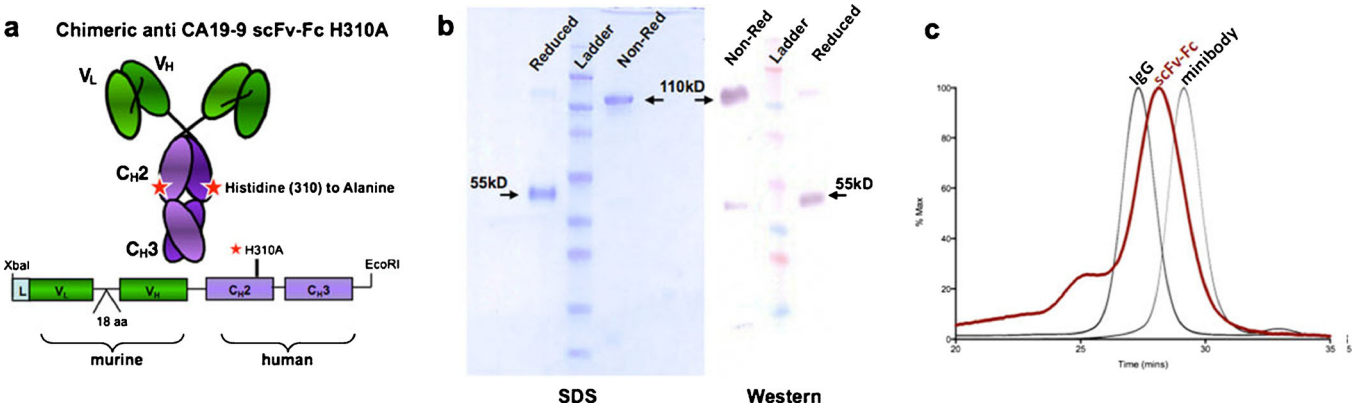

Fig. 1. **a** Schematic of the DNA construct and resulting protein dimmer of the chimeric anti-CA19-9 scFv-Fc with mutation site. **b** SDS-PAGE and Western blot of purified protein under reducing and nonreducing conditions. **c** Size-exclusion chromatography demonstrating the intermediate size of the anti-CA19-9 scFv-Fc H310A fragment (105 kDa) compared to an intact IgG (150 kDa) and a minibody (80 kDa).

Expression, Selection, and Purification

Utilizing electroporation, 1×10^7 NS0 murine myeloma cells (Lonza Biologics) were transfected with 40 μg of the pEE12 vector containing the scFv-Fc construct. The transfected NS0 cells were selected in glutamine-deficient DMEM/high modified media (JRH Biosciences, Lenexa, KS) as previously described [20, 21]. Cell culture supernatants were assayed by Western blot and probed using alkaline phosphatase (AP)-conjugated goat anti-human IgG Fcγ specific (Jackson ImmunoResearch, West Grove, PA), at a 1:5,000 dilution. The AP was developed with BCIP and NBT (Bio-Rad) in 10 ml of AP buffer per the manufacturer's recommendations. This allowed for selection of high expression clones, which were then expanded into triple flasks (Nunclon, Rochester, NY), and cultured to exhaustion. Supernatant was harvested, sterile-filtered with a 0.20-μm filter (Sartorius Stedim Biotech, Goettingen, Germany), and purified using an AKTA Purifier (Amersham Biosciences AB, Uppsala, Sweden) via affinity chromatography using a 10 ml Protein G column (Applied Biosystems, Carlsbad, CA). Fractions containing the protein of interest were pooled and dialyzed against 4 l of phosphate buffered saline (PBS) in a Slide-A-Lyzer Dialysis Cassette (Thermo Fisher Scientific, Rockford, IL) three consecutive times and then concentrated in Vivaspin 20 concentrating columns (Sartorius Stedim). The final concentration was determined by measuring absorbance at A_{280nm} on a NanoDrop 2000 Spectrophotometer (Thermo Fisher Scientific) using an extinction coefficient of ε=1.4.

Characterization

Purified protein was analyzed by sodium dodecyl sulfate polyacrylamide gel electrophoresis (SDS-PAGE) and Western blot under reducing (1 mM dithiothreitol) and nonreducing conditions and run on precast 4–20 % polyacrylamide ready gels (Bio-Rad Laboratories, Hercules, CA). The SDS was developed with Instant Blue (Expedeon, San Diego, CA), while the Western blot was probed using alkaline phosphatase (AP) conjugated goat anti-human IgG Fcγ specific as described above.

Purified protein was subjected to size-exclusion chromatography (SEC) on a Superdex 200 HR 10/30 column (Amersham) run isocratically in PBS. A 100-μl volume containing 50 μg of pure protein was loaded onto the column and eluted at 0.5 ml/min flow rate. Elution time was compared to a commercially available intact IgG, trastuzumab (Herceptin) [22, 23], and a well-characterized minibody A11 anti-PSCA (80 kDa) [24].

The CA 19-9 antigen-binding capability of the scFv-Fc H310A was analyzed via flow cytometry. BxPC3 pancreatic cancer cells which express approximately 1×10^6 epitopes per cell were utilized as the positive cell line, while MiaPaca-2 which has negligible cell surface expression was utilized as the negative cell line [14]. From culture, 2×10^5 cells were harvested and resuspended in 250 μl of PBS/1 % fetal bovine serum (FBS). The antibody was added in abundance (4 μg) and incubated for 1 h. Following the incubation, the samples were washed in 250 μl of PBS/1 % FBS and resuspended in 250 μl of PBS/1 % FBS. The secondary antibody and fluorescein isothiocyanate (FITC) conjugated goat anti-human IgG Fc specific (Jackson ImmunoResearch) antibody (1 μg) was incubated with each sample for 1 h and was similarly washed and resuspended. Negative controls included cells only, and cells and secondary antibody only. Positive control included cells incubated with intact anti-CA19-9 antibody (Invitrogen, Carlsbad, CA) followed by incubation with FITC-conjugated anti-mouse IgG Fc specific (Jackson ImmunoResearch).

The affinity of the scFv-Fc H310A was assessed by cell-based ELISA. From culture, 5×10^4 BxPC3 cells were harvested and added to each well of a 96-well V-bottom plate (Costar, Corning, NY). The cells were washed and resuspended in 100 μl of increasing concentrations of scFv-Fc H310A from 0 to 512 nM and incubated for 1 h at 4 °C. Following incubation, the cells were washed in 150 μl of PBS/1 % FBS and incubated in 100 μl of AP-goat anti-human IgG Fc specific antibody (Jackson ImmunoResearch) at a 1:1,000 dilution for 1 h. The cells were again washed and developed with phosphatase substrate tablets (Sigma) in diethanolamine buffer. Absorbance was measured on a GENios ELISA plate reader (Tecan, Switzerland) at 405 nm. All measurements were performed in triplicate.

Radioiodination

Radioiodination with the positron-emitting isotope ^{124}I was accomplished by the Iodo-Gen method as previously described

[20]. Labeling reactions (0.1–0.2 ml) typically contained 0.1 to 0.2 mg purified protein and 0.5–1.0 mCi $Na^{124}I$ (IBA Molecular, Dulles, VA). Labeling efficiency was measured by instant thin layer chromatography (TLC) (Biodex Medical Systems, Shirley, NY). Immunoreactivity was determined by incubating the radioiodinated scFv-Fc H310A fragment diluted to approximately 30,000 counts per minute (CPM) with BxPC3 cells such that there was an abundance of antigen. After incubation for 1 h, supernatant was collected, the pellet was resuspended, and both were measured for radioactivity in CPM by a Wizard 3" 1480 Automatic Gamma Counter (Perkin-Elmer Covina, CA). The immunoreactive fraction was determined by use of the following equation: cells radioactivity/(supernatant radioactivity+cells radioactivity).

Pharmacokinetics

All animal handling was performed under a protocol approved by the Chancellor's Animal Research Committee of UCLA. Eight-week-old female nude mice were obtained from Charles Rivers Laboratories (Wilmington, MA). The mice were injected with 25 μg of ^{124}I-anti-CA 19-9 scFv-Fc H310A labeled with 165 μCi of radioactivity in sterile normal saline (Abraxis, Shaumburg, IL) via the tail vein. Following injection, 5 μl of blood was collected from the tail vein at each of 11 time points ranging from 0.1 to 48 h. Radioactivity in each 5-μl sample was counted in a gamma counter for analysis. Radioactivity was converted to a percentage of the injected dose per gram of blood (%ID/g). Results were plotted as a two-phase decay curve on Prism 5 for Mac (GraphPad Software Inc., La Jolla, CA), and a terminal half-life ($t_{1/2\beta}$) was calculated.

Xenograft Imaging and Biodistribution Studies

Human tumor xenografts were established in 8-week-old female nude mice. Approximately 1×10^6 cells of the antigen-positive (BxPC3) or antigen-negative (MiaPaca-2) cancer cell lines were injected subcutaneously on the left and right shoulder, respectively, and allowed to grow for 14–21 days before imaging. The orthotopic tumor models were established by transplantation of a 1-mm BxPC3 solid tumor cube into the distal pancreas. The procedure involved creating a 1-cm incision over the left flank of the anesthetized mice. The spleen and distal pancreas were delivered through this incision into the operating field. A small pocket in the distal pancreas was carefully created with blunt dissection. The 1-mm tumor cube was then sutured into this pocket in the distal pancreas with a 4.0 nylon suture. Hemostasis was achieved with delicate pressure (cotton tip applicator), and the tumor, pancreas, and spleen were returned to the abdominal cavity. The abdominal incision was then closed in two layers utilizing a 4.0 absorbable suture. Mice were allowed to recover from anesthesia under close monitoring, and the implanted tumors were allowed to grow for 21–24 days before imaging. Saturated potassium iodide (0.5 ml per 100 ml water) was added to the drinking water 48 h prior to injection to block thyroid uptake of radioactive iodine. Gastric lavage with 1.5 mg of potassium perchlorate in 200 μl of PBS was performed 30 min prior to tail vein injection to block stomach uptake.

Mice in the subcutaneous model were injected with 12.5 μg of ^{124}I-scFv-Fc H310A (specific activity of 8.8±0.2 μCi/μg) in sterile normal saline (Abraxis) via the tail vein. Mice in the orthotopic model were injected with 20–25 μg of the ^{124}I-scFv-Fc H310A (specific activity of 4.2±0.3 μCi/μg). At 4, 24, and 48 h postinjection, the mice were anesthetized using 2 % isoflurane, placed on the micro-positron emission tomography (microPET) bed, and imaged with a Focus microPET scanner (Concorde Microsystems Inc., Knoxville, TN). Acquisition time was 10 min. All images were reconstructed by nonattenuation or scatter-corrected filtered back projection and displayed by the AMIDE software package [25, 26]. Animals were also imaged by micro-computed tomography (microCT) (ImTek Inc., Knoxville, TN) with the resultant images coregistered with the microPET scans for anatomic reference. Following the final time point, animals were euthanized; blood was collected by cardiac puncture and weighed; tumors, organs, muscle, and carcass were also harvested and weighed. Radioactive uptake of organs was counted in a gamma counter for biodistribution analysis. After decay correction, radioactive uptake in organs was converted to percentage of injected dose per gram of tissue (%ID/g) and statistical differences in uptake were determined by paired *t* test, after ensuring that the data was normally distributed (GraphPad Prism), results were considered significant at $p\leq0.05$.

Results

Production, Purification, and Characterization

The anti-CA 19-9 scFv-Fc H310A antibody was expressed in murine NS0 myeloma cells. Clones producing the highest amount of antibody by Western blot were selected for expansion. The antibody yield from triple flask supernatant was approximately 22 mg/l. Antibody purity was confirmed by standard SDS-PAGE under reducing and nonreducing conditions (Fig. 1b). Western blot probing for the human Fc region confirmed the protein identity. The scFv-Fc H310A (105 kDa) fragment had an elution time on a size-exclusion chromatography column of 28.1 min between that of the intact Herceptin IgG (150 kDa) and the well-characterized A11 minibody (80 kDa) standards confirming its intermediate size (Fig. 1c); the preceding shoulder of the scFv-Fc H310A curve represents a small percentage of noncovalent high molecular weight aggregates of the antibody fragment. Compared to the intact murine parental antibody, the scFv-Fc H310A fragment displayed similar binding of positive cell line (BxPc3) on flow cytometry. Cell-based ELISA estimated the equilibrium binding affinity constant (K_D) of the scFv-Fc H310A fragment to be 10.7±3.8 nM (Fig. 2). This is within the range of prior publications of the affinity constant for the intact parental antibody [14]. The pharmacokinetics of the mutated fragment was determined by injecting mice with ^{124}I-scFv-Fc H310A and performing serial measurements of remaining radioactivity in tail vein blood. The antibody fragment terminal half-life ($t_{1/2\beta}$) as determined by a two-phase decay nonlinear regression was 8.7 h (Fig. 2).

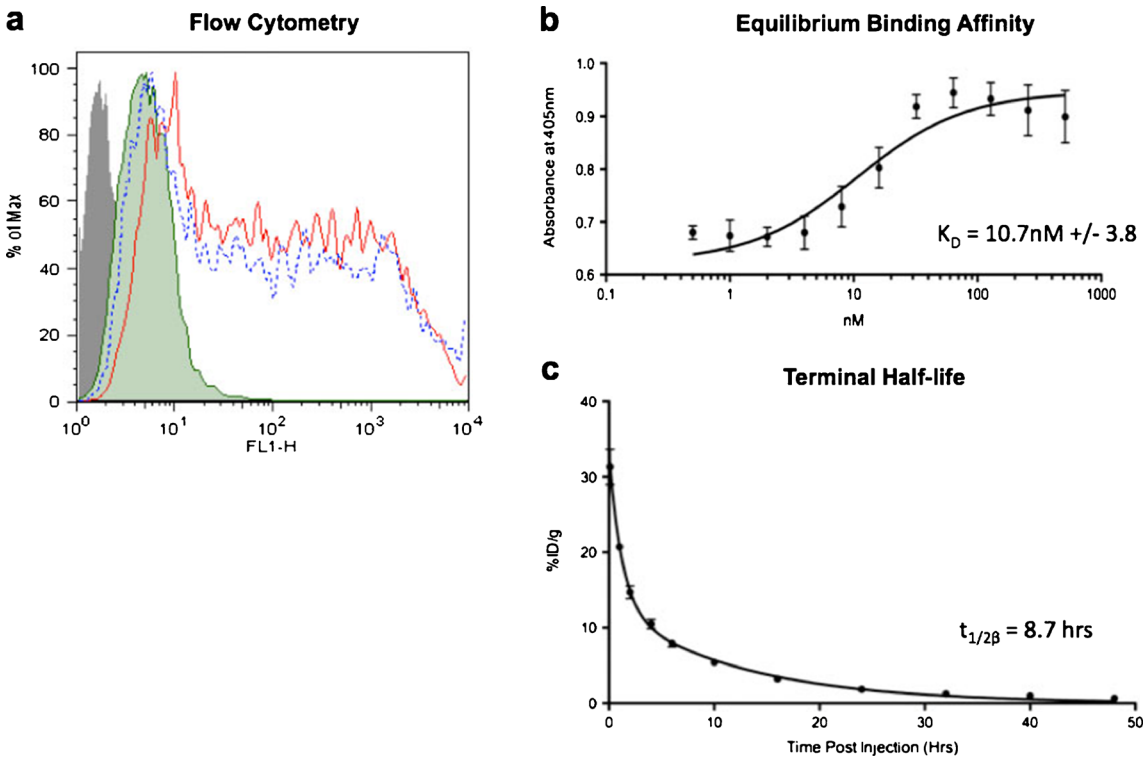

Fig. 2. **a** Flow cytometry demonstrating antigen-specific binding: BxPC3 human pancreatic cells only (*gray-filled*), cells with FITC secondary only (*green-tinted*), 500 nM of scFv-Fc H310A fragment (*red solid line*), and 500 nM of parental intact antibody (*blue dashed line*). **b** Equilibrium-binding affinity constant (K_D) as determined by cell-based ELISA. **c** Terminal half-life ($t_{1/2\beta}$) as determined by a nonlinear regression of two-phase decay.

Radioiodination, Xenograft Imaging, and Biodistribution Studies

Subcutaneous Model

Radioiodination with ^{124}I was performed with a labeling efficiency of 92.8 %. Immunoreactivity was 50.6 %. Four nude mice harboring CA 19-9 antigen-positive (BxPC3) and antigen-negative tumors (MiaPaca-2) were injected with 12.5 μg of scFv-Fc H310A with an average specific activity of 8.8 μCi/μg. Average tumor weight for BxPC3 tumors was 158 mg (range 46–377 mg), while the MiaPaca-2 tumors were 74 mg (range 43–147). Whole body microPET and microCT scans were obtained at 4, 24, and 48 h postinjection. Fig. 3 illustrates the composite PET/CT images from a representative animal at all three time points. The images indicate specific uptake of the radiolabeled scFv-Fc H310A antibody fragment to the antigen-positive tumor on the left shoulder. There is minimal background activity visualized by microPET at the 24- and 48-h time points. Fig. 3 also shows the biodistribution results after 48 h expressed as the percent of injected dose per gram of tissue (%ID/g) for the blood, tumors, and organs to provide objective confirmation of the microPET images. The uptake (%ID/g±SD) in the antigen-positive BxPC3 tumors was 2.78±1.42, while in the antigen-negative MiaPaca-2 tumors, it was 0.12±0.06. The average %ID/g in the blood was 0.22±0.06 and the liver was 0.66±0.50. The difference between the uptake in the antigen-positive tumor and the blood (p=0.03), antigen-negative tumor (p=0.03), and liver (p=0.05) all reached statistical significance on paired t test. The average tumor-to-blood ratio for the antigen-positive BxPC3 tumors was 13:1 with an average positive tumor-to-negative tumor ratio of 23:1 at 48 h.

Orthotopic Model

Radioiodination with ^{124}I was performed with a labeling efficiency of 89–99 %. Immunoreactivity was 30.2–55.6 %. Eight nude mice harboring CA 19-9 positive tumors (BxPC3) orthotopically established in the tail of the pancreas were injected via the tail vein with 20–25 μg of antibody with an average specific activity of 4.6 μCi/μg. The average tumor weight for the orthotopically implanted tumors was 157 mg (range 51–335 mg). Whole body microPET and microCT scans were obtained at 24 and 48 h. Fig. 4 illustrates the composite PET/CT images from all eight animals imaged at both time points as well as the necropsy images demonstrating the presence of tumor in the tail of the pancreas. Images shown indicate specific uptake of scFv-Fc H310A antibody fragment to the orthotopically implanted tumor. There is minimal background activity on microPET at 48 h allowing visualization of the tumor within the

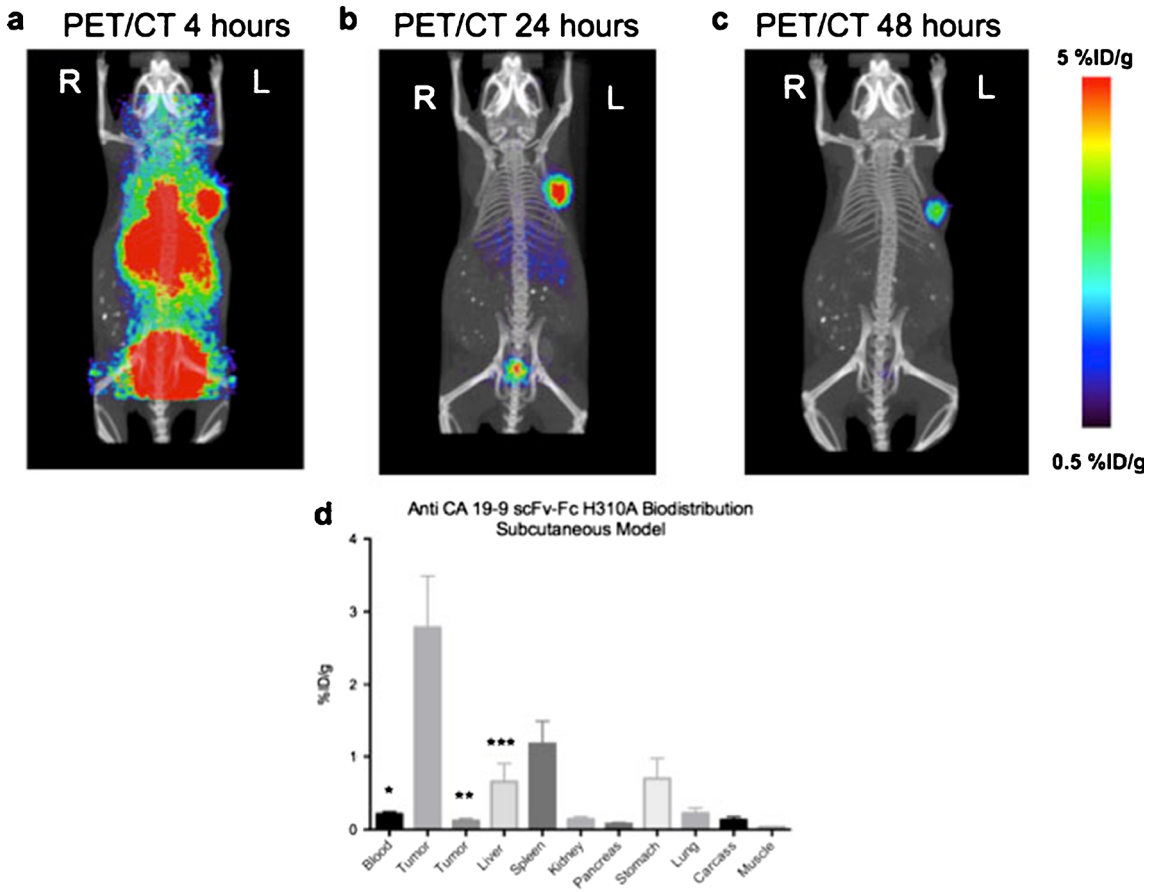

Fig. 3. Representative composite PET/CT images from a mouse at **a** 4 h, **b** 24 h, and **c** 48 h after injection of ^{124}I-labeled anti-CA19-9 scFv-Fc H310A fragment. All PET/CT images are scaled to the same threshold to allow for comparison across time points. **d** Biodistribution data demonstrating significantly increased uptake of radioactivity into the antigen-positive tumor compared to the blood (*asterisk*), antigen-negative tumor (*double asterisk*), and the liver (*triple asterisk*) after 48 h; *error bars* represent the standard error of the means.

abdominal cavity in seven of the eight mice. The mouse that did not demonstrate targeting was noted at the time of necropsy to have a tumor that under gross inspection was more fibrotic and did not appear consistent with the other seven tumors, and this is evident in the necropsy images. The tumor weights, tumor uptake, and tumor-to-blood ratios for all eight mice are also displayed in Fig. 4. Fig. 5 shows a graphical representation of the average %ID/g for the blood, tumors, and organs of all eight mice to provide objective confirmation of the microPET images. The average uptake (%ID/g±SD) in the antigen-positive BxPC3 tumors was 1.28±0.67, while in the blood it was 0.52±0.26, and the liver was 0.53±0.24. The difference between the uptake in the tumor and the blood (p=0.02) and liver (p=0.01) reached statistical significance on paired t test. The average tumor-to-blood ratio for the BxPC3 tumors was 2.5:1 at 48 h.

Discussion

Pancreatic cancer continues to be a devastating diagnosis for patients; it has a mortality that approximates its incidence, despite significant advances in medical and surgical treatment of the disease [1]. Pancreatic cancer is routinely understaged due to our inability to accurately image the extent of disease. Patients staged by our current imaging modalities with only localized disease are candidates for surgical resection and potential cure. Unfortunately, as evidenced by postoperative survival data, the majority of these patients have metastatic disease which is undetectable by our current imaging modalities [6, 27]. This demonstrates the desperate need for tumor-specific imaging agents as well as targeted therapeutics to improve outcomes and reduce the toxicity associated with current systemic chemotherapeutics [28, 29].

Our laboratory has sought to develop an antibody fragment, which can serve as an imaging agent with the potential to be further developed into a targeted therapeutic agent. Our fragment of interest is the domain-deleted scFv-Fc due to its stability, ease of production, and the modifiable nature of the intact Fc region. This fragment, and our ability to modulate its pharmacokinetic profile through site-specific mutations in the Fc region, offers significant advantages for transforming an imaging agent into a potential therapeutic.

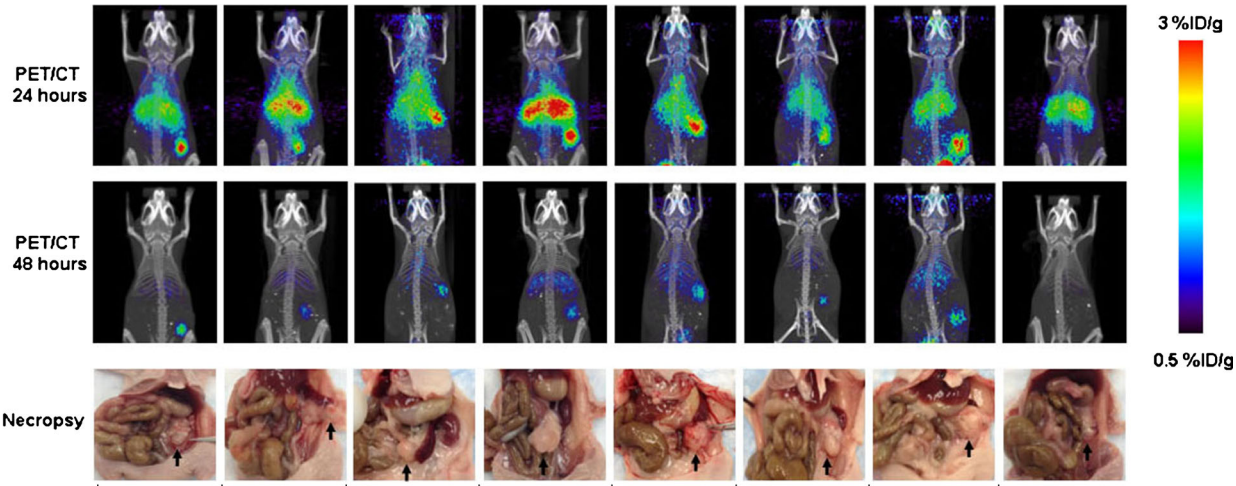

Tumor Weight (mg)	51	76	115	123	251	176	335	127
Tumor Uptake (%ID/g)	2.46	1.62	1.38	1.55	1.42	0.85	0.67	0.30
Tumor to Blood Ratio	8.8	2.7	1.7	4.6	1.5	2.0	1.4	1.3

Fig. 4. Representative composite PET/CT images from all eight mice at 24, 48 h, and during necropsy following injection of ^{124}I-labeled anti-CA19-9 scFv-Fc H310A fragment. *Arrow* denotes the location of orthotopic tumor. All PET/CT images are scaled to the same threshold to allow for comparison between mice and across all time points. Tumor weight (mg), tumor uptake (%ID/g), and tumor-to-blood ratios are also expressed for the corresponding mice images.

An intact antibody has a prolonged serum half-life secondary to FcRn receptor-mediated recycling following endocytosis instead of direction to the lysosome for degradation [30, 31]. For imaging, this recycling creates an elevated background signal, requiring a longer circulation time from injection of the radiolabeled antibody until the time at which a clinically useful image can be obtained. In the present study, we manipulated a scFv-Fc antibody fragment by altering the histidine at position 310 to an alanine so that it may better perform as an imaging agent by preventing antibody recycling and reducing serum persistence.

Functional and biochemical characterization was performed on the newly created anti-CA 19-9 scFv-Fc H310A fragment. This confirmed that the fragment created was of the expected size (105 kDa) and that it was a chimeric fragment bearing a human Fc region. Furthermore, the antibody fragment displayed antigen specificity for CA 19-9 positive cells by binding to the antigen-positive BxPc3cell line on flow cytometry. On cell-based ELISA, the scFv-Fc H310A antigen affinity was comparable to that of the parental intact murine monoclonal antibody (K_D=10.7 versus the published affinity of 12–15 nM for the intact antibody [14]). Based on these results, we proceeded with *in vivo* evaluation of our fragment.

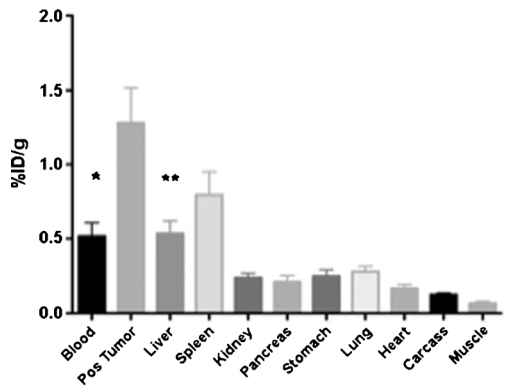

Fig. 5. Biodistribution of anti-CA19-9 scFv-Fc H310A demonstrating significantly increased uptake of radioactivity into the antigen-positive tumor compared to the blood (*asterisk*) and liver (*double asterisk*) after 48 h; *error bars* represent the standard error of the means.

Pharmacokinetic studies utilizing ^{124}I-labeled scFv-Fc H310A fragments were conducted to assess the serum clearance. The serum terminal half-life of the mutated antibody fragment in a nontumor-bearing nude mouse was 8.7 h. This terminal half-life for the CA19-9 scFv-Fc H310A fragment is somewhat shorter than previously published half-life data for an anti-carcinoembryonic antigen (CEA) scFv-Fc H310A fragment, which was described as 27.2 h [20]. This difference may be due to the fact that the CEA fragments' half-life was established in immunocompetent BALB/c mice, while the CA19-9 fragments half-life was established in immunocompromised nude mice. These results are also consistent with the findings by Kim *et al.* that the histidine to alanine mutation at position 310 confers an estimated 93 % reduction in FcRn binding affinity [16].

Not only were we able to modify the pharmacokinetics of this fragment without affecting its *in vitro* binding affinity but we also demonstrated that the mutated scFv-Fc H310A antibody fragment targeted pancreatic tumors *in vivo*. Imaging and biodistribution studies were conducted in nude mice harboring an antigen-positive pancreatic cancer tumor xenograft (BxPC3) on the left shoulder and an antigen-negative pancreatic cancer tumor xenograft (MiaPaca 2) on the right shoulder so that each mouse could serve as its own

control. The images displayed show excellent tumor uptake of radioactivity at 24 h with clear discrimination of the tumor from background. The 48-h image demonstrates decreased background signal due to the enhanced serum clearance of the scFv-Fc H310A fragment. This allows for improved image contrast after only 48 h compared to that obtained with the intact antibody after 120 h; this improved contrast is also supported by the objective confirmation on biodistribution of a tumor-to-blood ratio of 13:1 obtained with the scFv-Fc H310A fragment at 48 h compared to the 5:1 ratio obtained with the intact antibody at 120 h [14]. The subcutaneous tumor model demonstrated antigen-specific tumor targeting and allowed comparison with our prior work with the intact antibody, but in order to more thoroughly assess our scFv-Fc H310A fragments' potential for translation to the patient, imaging a model that more closely recapitulates human pancreatic cancer was necessary.

Therefore, we developed an orthotopic human pancreatic cancer model via surgically transplanting CA 19-9 antigen-positive human pancreatic cancer tissue into the distal pancreas of nude mice. Using this model, we were able to assess the ability of this fragment to generate the required contrast to visualize a tumor within the abdomen from the blood and liver background signal. As in the subcutaneous model, the images displayed show adequate tumor discrimination at 48 h. The biodistribution data also demonstrated that the %ID/g uptake in the tumor was significantly higher than the uptake in the liver ($p=0.01$) as well as the blood background ($p=0.02$). With objective evidence of targeting based on biodistribution data coupled with microPET images of both the subcutaneous and orthotopic tumor models, we demonstrate the utility of the anti CA19-9 scFv-Fc H310A fragment as a PET imaging agent in regard to providing antigen-specific imaging at earlier time points compared with the intact antibody.

In summary, the use of molecular imaging techniques such as immunoPET provide the opportunity for more accurate assessment of the extent of disease in pancreatic cancer patients and may be able to minimize the morbidity and mortality of unsuccessful attempts at resection and guide treatment decisions. Furthermore, as the field of immunoPET and immunotherapy evolves, antibody fragments such as our domain-deleted single-chain Fv-Fc, with modifiable pharmacokinetics, may lead to tumor-specific imaging agents that can easily be translated into immunotherapeutics. In this study, we created a scFv-Fc antibody fragment with a decreased serum half-life through a site-directed mutation in the Fc region. We assessed its biologic and biochemical properties and its utility as an imaging agent. Our mouse models of pancreatic cancer demonstrate that not only does the fragment demonstrate antigen specificity *in vivo* but is also capable of imaging orthotopic pancreatic cancer in spite of abdominal background signal. Further investigation will be directed towards modifying anti CA19-9 scFv-Fc fragments whose pharmacokinetic profile may make them more ideal for therapeutic applications such as radioimmunotherapy.

Acknowledgments. This study was supported in part by a VA Carreer Development Award (J Tomlinson) VA0002. Additionally, the authors would like to acknowledge the UCLA Jonsson Comprehensive Cancer Center grant P30 CA016042 and the CFAR grant 5P30 AI028697 for support of the flow cytometry assays performed in this study.

Conflict of Interest. The authors do not have any conflicts of interest to disclose for this manuscript.

References

1. American Cancer Society (2012) Cancer facts & figures. American Cancer Society, Atlanta
2. Winter JM, Cameron JL, Campbell KA et al (2006) 1423 pancreaticoduodenectomies for pancreatic cancer: a single-institution experience. J Gastrointest Surg 10:1199–1210, discussion 1210-1191
3. Siegel R, Naishadham D, Jemal A (2012) Cancer statistics, 2012. CA Cancer J Clin 62:10–29
4. Mancuso A, Calabro F, Sternberg CN (2006) Current therapies and advances in the treatment of pancreatic cancer. Crit Rev Oncol Hematol 58:231–241
5. Richter A, Niedergethmann M, Sturm JW et al (2003) Long-term results of partial pancreaticoduodenectomy for ductal adenocarcinoma of the pancreatic head: 25-year experience. World J Surg 27:324–329
6. Wasif N, Ko CY, Farrell J et al (2010) Impact of tumor grade on prognosis in pancreatic cancer: should we include grade in AJCC staging? Ann Surg Oncol 17:2312–2320
7. Knowles SM, Wu AM (2012) Advances in immuno-positron emission tomography: antibodies for molecular imaging in oncology. J Clin Oncol 30:3884–3892
8. Scott AM, Wolchok JD, Old LJ (2012) Antibody therapy of cancer. Nat Rev Cancer 12:278–287
9. Haglund C, Lindgren J, Roberts PJ, Nordling S (1986) Gastrointestinal cancer-associated antigen CA 19-9 in histological specimens of pancreatic tumours and pancreatitis. Br J Cancer 53:189–195
10. Loy TS, Sharp SC, Andershock CJ, Craig SB (1993) Distribution of CA 19-9 in adenocarcinomas and transitional cell carcinomas. An immunohistochemical study of 527 cases. Am J Clin Pathol 99:726–728
11. Makovitzky J (1986) The distribution and localization of the monoclonal antibody-defined antigen 19-9 (CA19-9) in chronic pancreatitis and pancreatic carcinoma. An immunohistochemical study. Virchows Arch B Cell Pathol Incl Mol Pathol 51:535–544
12. Atkinson BF, Ernst CS, Herlyn M et al (1982) Gastrointestinal cancer-associated antigen in immunoperoxidase assay. Cancer Res 42:4820–4823
13. Chang TH, Steplewski Z, Sears HF, Koprowski H (1981) Detection of monoclonal antibody-defined colorectal carcinoma antigen by solid-phase binding inhibition radioimmunoassay. Hybridoma 1:37–45
14. Girgis MD, Olafsen T, Kenanova V et al (2011) CA19-9 as a potential target for radiolabeled antibody-based positron emission tomography of pancreas cancer. Int J Mol Imaging 2011:834515
15. Girgis MD, Olafsen T, Kenanova V et al (2011) Targeting CEA in pancreas cancer xenografts with a mutated scFv-Fc antibody fragment. EJNMMI Res 1:24
16. Kim JK, Firan M, Radu CG et al (1999) Mapping the site on human IgG for binding of the MHC class I-related receptor, FcRn. Eur J Immunol 29:2819–2825
17. Shields RL, Namenuk AK, Hong K et al (2001) High resolution mapping of the binding site on human IgG1 for Fc gamma RI, Fc gamma RII, Fc gamma RIII, and FcRn and design of IgG1 variants with improved binding to the Fc gamma R. J Biol Chem 276:6591–6604
18. Girgis MD, Kenanova V, Olafsen T et al (2011) Anti-CA19-9 diabody as a PET imaging probe for pancreas cancer. J Surg Res 170:169–178
19. Wu AM, Yazaki PJ (2000) Designer genes: recombinant antibody fragments for biological imaging. Q J Nucl Med 44:268–283
20. Kenanova V, Olafsen T, Crow DM et al (2005) Tailoring the pharmacokinetics and positron emission tomography imaging properties of anti-carcinoembryonic antigen single-chain Fv-Fc antibody fragments. Cancer Res 65:622–631
21. Galfre G, Milstein C (1981) Preparation of monoclonal antibodies: strategies and procedures. Methods Enzymol 73:3–46
22. Yu D, Hung MC (2000) Overexpression of ErbB2 in cancer and ErbB2-targeting strategies. Oncogene 19:6115–6121

23. Hudis CA (2007) Trastuzumab–mechanism of action and use in clinical practice. N Engl J Med 357:39–51
24. Lepin EJ, Leyton JV, Zhou Y et al (2010) An affinity matured minibody for PET imaging of prostate stem cell antigen (PSCA)-expressing tumors. Eur J Nucl Med Mol Imaging 37:1529–1538
25. Defrise M, Kinahan PE, Townsend DW et al (1997) Exact and approximate rebinning algorithms for 3-D PET data. IEEE Trans Med Imaging 16:145–158
26. Loening AM, Gambhir SS (2003) AMIDE: a free software tool for multimodality medical image analysis. Mol Imaging 2:131–137
27. Wasif N, Bentrem DJ, Farrell JJ et al (2010) Invasive intraductal papillary mucinous neoplasm versus sporadic pancreatic adenocarcinoma: a stage-matched comparison of outcomes. Cancer 116:3369–3377
28. Picozzi VJ, Abrams RA, Decker PA et al (2011) Multicenter phase II trial of adjuvant therapy for resected pancreatic cancer using cisplatin, 5-fluorouracil, and interferon-alfa-2b-based chemoradiation: ACOSOG Trial Z05031. Ann Oncol 22:348–354
29. Vaccaro V, Sperduti I, Milella M (2011) FOLFIRINOX versus gemcitabine for metastatic pancreatic cancer. N Engl J Med 365:768–769, author reply 769
30. Junghans RP, Anderson CL (1996) The protection receptor for IgG catabolism is the beta2-microglobulin-containing neonatal intestinal transport receptor. Proc Natl Acad Sci U S A 93:5512–5516
31. Israel EJ, Wilsker DF, Hayes KC et al (1996) Increased clearance of IgG in mice that lack beta 2-microglobulin: possible protective role of FcRn. Immunology 89:573–578